

Nutrient Flows and Biogeomorphic Feedbacks: Linking Seabird Guano to Plant traits and Morphological Change on Sandy Islands

Floris F. van Rees^{1,2,3}, Laura L. Govers^{1,4}, Polina Guseva², Maarten P.A. Zwarts², Camille Tuijnman², Cornelis J. Camphuysen¹, Gerben Ruessink², Valérie C. Reijers²

5 ¹ Department of Coastal Systems, Royal Netherlands Institute for Sea Research (NIOZ), 't Horntje, 1797 SZ, the Netherlands;

² Department of Physical Geography, Utrecht University, Utrecht, 3584 CS, the Netherlands

³ Department of Ecosystems and Sediment Dynamics, Deltares, Delft, 2629 HV, the Netherlands

10 ⁴ Groningen Institute for Evolutionary Life Sciences (GELIFES), University of Groningen, 9700 CC, Groningen, the Netherlands

Correspondence to: Floris F. van Rees (floris.van.rees@nioz.nl)

Abstract. Vegetated coastal landscapes are crucial for carbon storage, shoreline protection, and biodiversity. Their structure emerges from biogeomorphic feedbacks between vegetation growth and sedimentation, shaped by environmental conditions. Allochthonous nutrient inputs, particularly seabird guano, can significantly influence plant growth and distribution, potentially altering these feedbacks. This suggests that coastal birds may actively shape their own habitat by modifying plant-sediment dynamics. Yet, as sea-level rise and coastal squeeze reduce available habitat for already declining bird populations, understanding these interactions becomes increasingly urgent, particularly on small, uninhabited islands that are geomorphically dynamic and whose nutrient budgets are dominated by allochthonous rather than locally produced nutrients. Despite this, spatially explicit studies on bird–plant–sediment interactions remain lacking. This study addresses that gap by examining how guano deposition influences plant traits, community composition, and landscape morphology. We combined fine-scale field data with remote sensing and spatial modelling to assess guano effects on vegetation and sedimentation. Field measurements included plant traits, community composition, environmental variables, and $\delta^{15}\text{N}$ to trace guano uptake. A guano dispersion model was linked to PlanetScope and LiDAR data, and Bayesian models (INLA) revealed spatial links between guano, vegetation change, and sediment accretion. Results show that guano-derived nitrogen promotes shifts in species composition toward later-successional, sediment-stabilizing species, particularly on sandy soils with low baseline nutrient levels. Guano enhanced early-season vegetation productivity, increasing sediment retention, but seasonal differences and local environmental context modulated these effects. We propose that seabirds act as indirect ecosystem engineers by fuelling vegetation–sediment feedbacks. Changes in breeding pair numbers may therefore influence coastal landscape evolution, and ultimately, shape the very habitats these birds depend on.

30

1 Introduction

Vegetated coastal landscapes play critical roles by storing carbon (Macreadie et al., 2019; McLeod et al., 2011), protecting coastlines from erosion and storms (Spalding et al., 2014), and supporting biodiversity (Sutton-Grier and Sandifer, 2019).

35 These coastal landscapes are biogeomorphic systems as they are shaped by reciprocal interactions between biological and physical processes (Corenblit et al., 2011). For instance, above-ground plant structures modulate wind or water flow, which promotes the trapping of sediments. Similarly, belowground plant structures like roots and rhizomes stabilise sediments by reducing lateral (De Battisti et al., 2019) and topsoil erosion (Marin-Diaz et al., 2021). These biological processes thus enhance surface accretion and shoreline stabilization, which in turn promote vegetation growth. The strength of these biogeomorphic
40 feedback interactions is dependent on the properties and behaviour of above- and below-ground plant structures, commonly referred to as plant traits. Dune grasses, for example, capture less sand with shorter, thinner or more flexible shoots compared to taller, thicker or stiffer ones (Van Boxel et al., 1999; Kuriyama et al., 2005; Zarnetske et al., 2012).

Plant trait expression is shaped both by species identity and by environmental context. First, different species possess inherently different plant traits. As environmental conditions change, such as through variations in sedimentation, moisture,
45 or salinity, so too can the composition of the vegetation community. In coastal dunes, for example, dynamic beach plains are typically colonised by burial- and overwash-tolerant pioneer species, while burial-intolerant, sediment-stabilizing shrubs are more common behind developed foredunes (Bakker et al., 2023; Woods and Zinnert, 2024). Because plant traits can influence aeolian and hydrodynamic sediment transport processes, shifts in species composition can have far-reaching consequences for coastal landscape morphodynamics (Schwarz et al., 2018). Second, environmental conditions can also influence intraspecific
50 trait expression. Marram grass (*Ammophila arenaria*; synonym *Calamagrostis arenaria*), for example, adapts its clonal expansion strategy in response to sedimentation to optimize sand capture (Reijers et al., 2021). In contrast, other dune- or marsh-forming species express relatively stable clonal traits across a range of environments (Lammers et al., 2023; van de Ven et al., 2023). Finally, biotic interactions, such as competition, grazing, or facilitation, can further modify plant trait expression, either by shifting community composition or directly altering key ecosystem-engineering plant traits like rooting depth or
55 vegetation height (Kim and Lee, 2022).

In addition to local drivers of environmental conditions and vegetation structure, vegetated coastal ecosystems, often located along gently sloping gradients, are strongly influenced by cross-ecosystem flows of water, energy, organisms, and nutrients between marine and terrestrial realms. Among these, nutrient flows can particularly profoundly affect plant productivity and trait expression, as well as broader ecosystem properties such as biodiversity, food web complexity and stability of food webs
60 (Polis et al., 1997). Especially on small islands where autochthonous production is small relative to allochthonous nutrient input from the sea (Anderson and Polis, 1999; Polis et al., 1997). Mobile consumers play a critical role in these transfers by actively redistributing nutrients across varying timescales, distances, and gradients in ways that abiotic processes alone cannot achieve (Bauer and Hoye, 2014; McInturf et al., 2019). Examples of these external nutrient pulses to coastal ecosystems include turtle nesting events on sandy shores (Le Gouvello et al., 2017), episodic deposition of washed-up wrack (Joyce et al., 2022),

65 seal feces released during birthing months (McLoughlin et al., 2016) and guano during the breeding season (Benkwitt et al., 2021; Buelow et al., 2018). These exchanges form part of the circular seabird economy, a framework describing how seabirds link oceans, islands, and nearshore habitats through repeated movement of marine-derived nutrients, thereby shaping both terrestrial and marine ecosystem functioning (Jones et al., 2023, 2025). In this manuscript, we use the term “seabirds” in a broad sense that also includes waders and shorebirds.

70 Especially guano is an important driver of local ecosystem productivity and biogeomorphic development on various island coastal landscapes, including island atolls (Dunn et al., 2025; Steibl et al., 2024), sandy barrier islands (Reijers et al., 2024), and mangrove ecosystems (Appoo and Bunbury, 2024). The incorporation of guano is often quantified using stable nitrogen isotopes, with elevated $\delta^{15}\text{N}$ levels indicating greater assimilation of nitrogen derived from higher trophic levels (Buelow et al., 2018; Maron et al., 2006; Reijers et al., 2024; Wainright et al., 1998). Guano can stimulate vegetation growth, but its effects are not universally positive; high nutrient loads can shift plant community composition, reduce species richness, or cause die-back under dry conditions, leading to trait changes that may or may not enhance soil stabilization (Anderson and Polis, 1999; Barrett et al., 2005; Ellis, 2005; Maron et al., 2006; Young et al., 2011). Therefore, biogeomorphic effects can be positive when guano-derived nutrients increase above and belowground biomass productivity, as this enhances sediment capture and erosion resistance (Dickey et al., 2023; Morton et al., 2025). On the other hand, guano fertilization can also weaken erosion resistance by reducing the selective pressure for below-ground foraging, leading to lower investment in root biomass (Marin-Diaz et al., 2021; Poorter & Nagel, 2000). So far, most studies assess the effects of bird guano on whole island ecosystem productivity by extrapolating findings on a few square meters to the whole island scale (Anderson et al., 2008; Ellis, 2005; Reijers et al., 2024), whereas local environmental conditions, such as differences in landscape morphology and hydrodynamic exposure, and spatial gradients in nutrient subsidy might differ strongly. This means that extrapolating plot-levels guano effects across whole-island scales can lead to inaccurate predictions, because the effect of fertilization is dependent on many environmental and biotic conditions that vary spatially and through time. These spatial differences can substantially shape biogeomorphic processes, influencing vegetation dynamics, sediment capture, and ultimately, the formation of bird habitat. As coastal ecosystems and their threatened avian inhabitants face mounting pressures from sea-level rise (van de Pol et al., 2024) and, on developed mainland coasts, coastal squeeze (Lansu et al., 2024), understanding how guano alters habitat structure at fine spatial scales is critical for conserving already declining bird populations (Palczny et al., 2015). This is key for identifying system-specific pathways, particularly on small sandy islands, through which seabirds can enhance vegetation–sediment feedbacks that contribute to shoreline stability.

Our study aims to disentangle the reciprocal relationships between guano, vegetation composition and traits, environmental conditions, and morphological changes on sandy biogeomorphic islands, where biological communities and geomorphic processes are tightly coupled through reciprocal feedbacks that allow organisms and landforms to co-shape each other (Stallins, 2006). To understand the role of bird-plant interactions in soft sediment coastal ecosystems, small uninhabited barrier islands offer a particularly informative setting, because of their dynamic geomorphology, and dependence on external nutrients. Combined with limited human interference, these islands create unique ecological niches that are particularly favourable for

seabird populations (Foster et al., 2009). We applied a multi-variable framework on two spatial levels on island in the Dutch
100 Wadden Sea. First, we characterised the (in)direct interactions between vegetation composition, plant trait expression, and the
environmental conditions on five sandy islands. This was conducted on a fine spatial resolution (4 m^2) with limited spatial
coverage using structural equation modelling that allows for integrating both direct and indirect effects, including spatial
dependency (Lefcheck, 2016). We hypothesize that plant trait expressions are influenced both directly and indirectly by guano
105 deposition and other abiotic factors. Secondly, we applied remote sensing techniques to investigate the interaction between
guano deposition, plant productivity and landscape morphological changes. We hypothesize that guano promotes vegetation
growth, thereby enhancing vegetation-driven sediment capture. This approach was performed on a coarser spatial resolution
(9 m^2) with a full island coverage using a Bayesian hierarchical joint modelling approach with an integrated nested Laplace
approximation to include a spatial correlation structure. Integrating fine-scale in situ monitoring with broad-scale remote
110 sensing provides a mechanistic understanding of biogeomorphic feedbacks (Cavender-bares et al., 2022; Lausch et al., 2018)
and elucidates the net effects of seabird guano on island morphology.

2 Methods

2.1 Sites description

Our study was performed on five uninhabited sandy islands situated in the Dutch Wadden Sea region, Rottumeroog (53°32'25"N, 6°34'55"E), Rottumerplaat (53°32'30"N, 6°28'51"E), Richel (53°17'50"N, 5°8'5"E), Griend (53°15'55"N, 5°15'15"E), and Zuiderduin (53°31'0"N, 6°35'0"E), (Figure 1). The Wadden Sea consists of vast tidal flats shielded by chains of barrier islands stretching 500 km from the Netherlands to Denmark (Kabat et al., 2012). The global significance of this region for millions of migratory birds has led to the Wadden Sea being designated as a UNESCO World Heritage Site. The tidal flats harbor a diverse community of benthic organisms (Compton et al., 2013), making it a vital foraging habitat for shorebirds (Boere and Piersma, 2012).

All islands are uninhabited, protected nature reserves that remain closed to the public year-round. They were selected because each island is sandy in origin, is shaped by feedback interactions between vegetation growth and sedimentation processes that drive their morphodynamic development, and harbours coastal bird colonies. Rottumeroog and Rottumerplaat are barrier islands, formed under wave-dominated conditions and shaped by aeolian processes that promote dune formation, which were affected by the construction of a sand drift dike around 1950. In contrast, Richel originated as an unvegetated sand shoal within the flood tidal delta. Since 2009, it has rapidly evolved into a vegetated sandy island, with dune development primarily driven by aeolian processes enabled by its long fetch. Zuiderduin separated from Rottumeroog around 1930 and has developed into a sandy back-barrier island (Reijers et al., 2024). Finally, Griend has existed since the Middle Ages but extensive erosion after 20th-century closure dam construction led to the construction of artificial stabilization of the island between 1980-1988. A 2016 sand nourishment (~200000 m³) was added to protect its critical breeding habitat, using locally dredged, nutrient-poor sand (Reijers et al., 2024).

The number of different breeding pairs and the number of species differ markedly between the islands (e.g., 1089 on Zuiderduin, 4519 on Rottumerplaat, 839 on Rottumeroog, 751 on Richel, and 9782 on Griend), reflecting the varying habitat conditions and management histories (Table S1 in the supplements). *Larus argentatus* (Herring Gull) and *Larus fuscus* (Lesser Black-backed Gull) dominate on all islands but are especially numerous on Rottumerplaat and Griend. *Chroicocephalus ridibundus* (Black-headed Gull) is only present on Zuiderduin and Griend, with a striking concentration on Griend. *Phalacrocorax carbo* (Great Cormorant) breeds on Zuiderduin and Richel, while *Larus canus* (Common Gull) is limited to Zuiderduin and Rottumeroog. Notably, Griend hosts the highest species diversity, including large colonies of *Thalasseus sandvicensis* (Sandwich Tern), *Platalea leucorodia* (Eurasian Spoonbill), *Sterna paradisaea* (Arctic Tern), and *Sterna hirundo* (Common Tern), which are absent from the other islands.

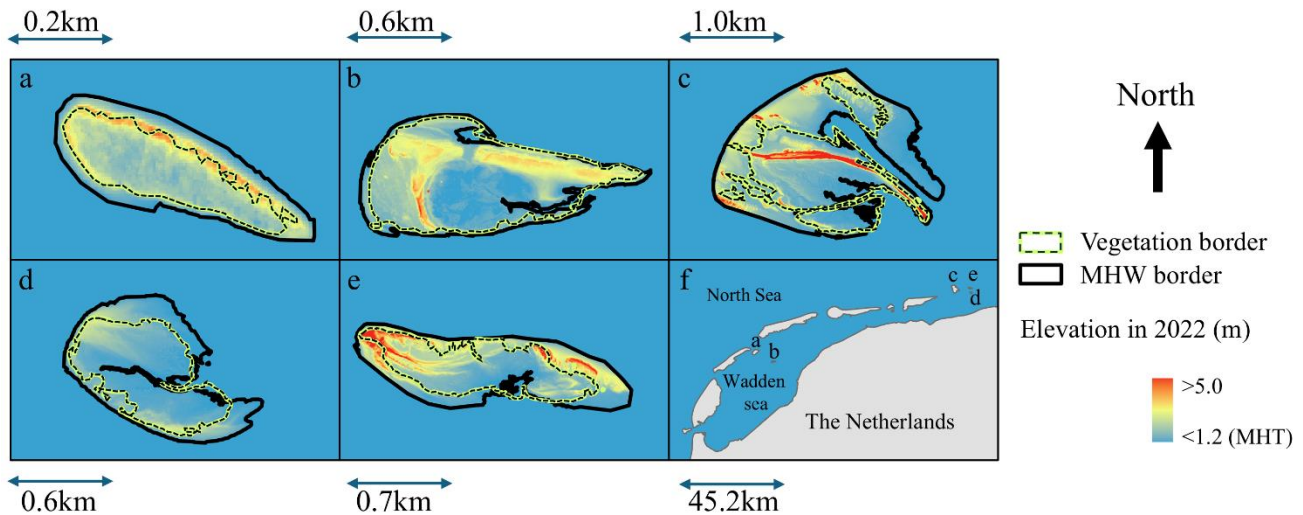


Figure 1: The five islands included in this study: Richel (a), Griend (b), Rottumerplaat (c), Zuiderduin (e), and Rottumeroog (e). Their relative location with respect to the mainland is displayed in panel (f). The colormap, elevation in 2022, shows the elevation with respect to the Dutch ordinance datum (NAP), based on LiDAR pointclouds (*Rijkswaterstaat, 2017*). The border of the vegetation is indicated by a green line with inner black dashed line defined as an NDVI higher than 0.2, as used in (Reijers et al., 2024), and the border of mean high tide (MHW) is depicted by a black line. On islands where MHW does not reach the vegetation border, tidal inundation does not contribute to sedimentation, instead sediment delivery to vegetated areas is predominantly steered by wind (a) or waves (d).

2.2 Study set-up

We used a two-tiered approach to examine how guano affects vegetation growth and sedimentation. First, we analysed guano effects on vegetation composition and plant traits using field measurements collected across the five islands. Second, we examined how spatial patterns in guano deposition correspond with island-scale variation in satellite-derived vegetation indices (NDVI, GI) and LiDAR-based elevation change (ΔZ) from 2021 to 2022. These two components are based on different spatial scales but capture complementary aspects of the same system and are used to investigate how small-scale field measurements in the field compare with island-scale remote sensing analyses. An overview of the methodology is provided in Figure 2.

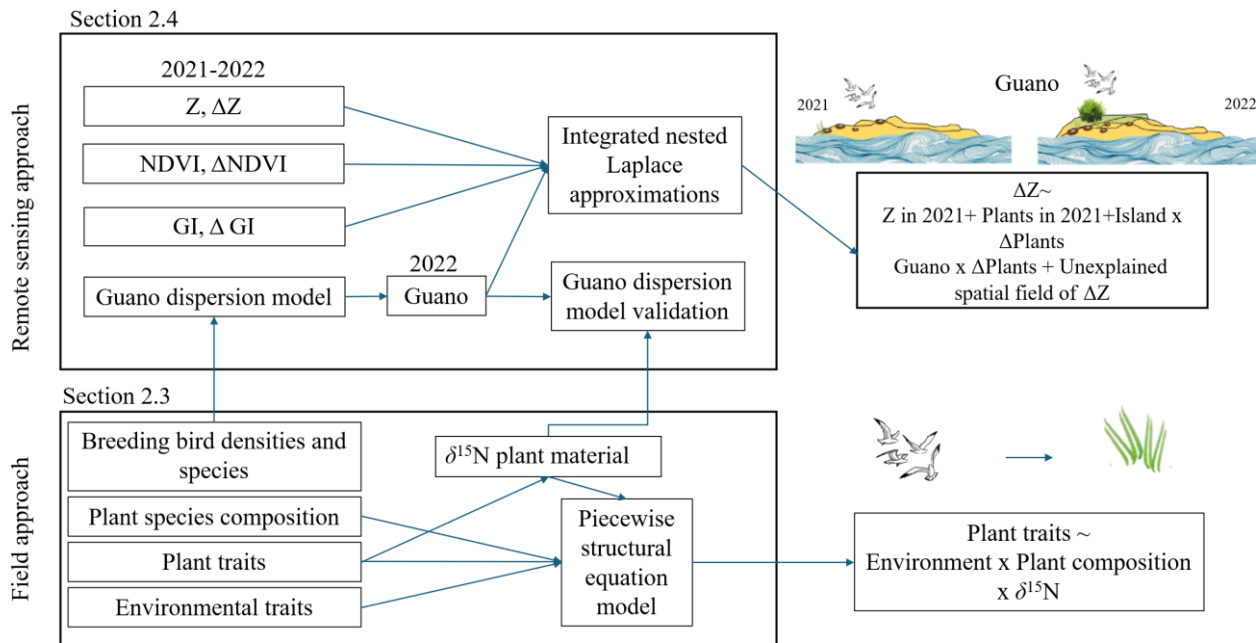


Figure 2: Schematic overview of the two-tiered methodological framework. Field approach: Structural equation modelling of how plant traits are driven by species composition, environmental conditions and foliar $\delta^{15}\text{N}$ (as a proxy for seabird-derived guano). Remote sensing approach: Island-wide Bayesian spatial modelling (INLA) of elevation change (ΔZ) in relation to vegetation state (NDVI, GI), its temporal changes (ΔNDVI , ΔGI) and guano deposition, with island-specific effects and spatial autocorrelation accounted for.

2.3 The effect of guano deposition on species composition and plant traits

On all five islands, we sampled vegetation composition, environmental conditions, and plant trait expression along transects ranging from 300 to 700 meters in length (5–6 sample plots per transect), resulting in 4–6 transect per island and 24–30 plots per island, 118 in total. Transect placement was designed to capture variation in guano deposition both within and outside bird colonies, while also encompassing environmental variability by sampling across pioneer and climax vegetation, and sandy and muddy substrates. As a result, transect lengths varied depending on the spatial configuration of colonies and the size of each island. On Richel and Rottumeroog, plot locations ($N = 30$ and $N = 29$, respectively) were distributed across the islands, as island width was insufficient to accommodate transect sampling, while still ensuring that a broad range of habitats and guano densities was sampled. Plots on transects were spaced evenly, and for each plot we choose a representative location based on surrounding vegetation and topography. Sampling was conducted in August and September 2022, shortly after the breeding season when guano deposition is at its annual peak and at the end of the plant growing season when vegetation has actively assimilated available nutrients, making guano–vegetation relationships likely most pronounced and detectable. At each

sampling plot, we identified plant species and estimated visually their percent cover within 2×2 m (4 m^2) plots to characterized the vegetation community composition following Lansu et al. (2025). Percent cover was visually estimated using 5% increments for most species. For species contributing less than 5% cover, we used 1% increments to record their presence while assigning proportionally low abundance. Vegetation was clipped within a 0.4×0.4 m frame placed in a representative area to determine plant biomass of the total community (g DW m^{-2}). Vegetation biomass was then determined after drying the samples at 60°C for 48 hours. Rooting depth was determined at each sampling plot as the average of two 1 m depth soil profiles (\varnothing 2.5 cm), placed beneath the dominant vegetation (or each of two co-dominant species), from which we measured the distance between the surface and the deepest living root. Vegetation height of the community was determined as the average of four measurements taken within a 10 cm radius of plot corners. Within each plot, we collected approximately five leaves from the three most abundant plant species to measure foliar carbon and nitrogen levels and the isotopic ratio of nitrogen ($\delta^{15}\text{N}$), which serves as a proxy for guano assimilation. Elevated $\delta^{15}\text{N}$ values ($\delta^{15}\text{N} > 10$) indicate that plants have incorporated organic nitrogen derived from guano (Maron et al., 2006; Reijers et al., 2024). This threshold was used only for interpretation and was not applied in any statistical modelling as $\delta^{15}\text{N}$ was analysed as a continuous variable. From the three species available per plot, we picked the species that was most common in all plots to decrease the number of different plant species measured. This was done to minimize the influence of species-specific nitrogen isotope fractionation. If the most common species was absent from a plot, the next most frequent species was selected, and this process was repeated as needed.

The plant samples for elemental analysis were initially rinsed with demineralized water, freeze-dried, and then finely ground and homogenized using a CG-200 Freezer/Mill Compact Cryogenic Grinder. Approximately 1 mg of each homogenized sample was placed into tin cups. These samples were analysed for $\delta^{15}\text{N}$ isotope ratios, using a Carlo-Erba NA-1500 Elemental Analyser coupled with a Thermo Finnigan DeltaPlus mass spectrometer via a Finnigan ConFlo III Universal Interface.

We also sampled environmental variables in each sampling plot. Included in our analysis were 1) soil organic matter content, 2) elevation relative to the Dutch ordnance datum (NAP), which is about mean sea level; and 3) distance from the coast. For soil organic matter, we collected sediment samples (100 mL) from the top 5 cm of soil. The organic matter content was then determined as loss on ignition by combusting dry sediment samples at 575°C for four hours (Heiri et al., 2001). Elevation was measured using a Topcon HiPer SR single RTK-GPS system. The distance from the coast was calculated as the Euclidean distance between each sampling point and the nearest cell in a raster indicating areas below mean high water in 2022. This elevation raster was derived from a LiDAR point cloud of the Dutch coast (Rijkswaterstaat, 2017).

To investigate how guano deposition affects the reciprocal relationships between environmental conditions, vegetation composition, and plant trait expression, we applied structural equation modelling (SEM) in R using the `piecewiseSEM` package (version 4.3.2). We used ordination techniques to reduce the dimensionality and capture key gradients into main axes for both the environmental variables, plant traits and vegetation community composition. For the environmental variables and the plant traits, we applied principal component analyses. The environmental PCA included mean elevation, distance from the coast, and soil organic matter content, whereas the plant-trait PCA was based on vegetation height, rooting depth, vegetation biomass, foliar carbon and nitrogen concentrations, and foliar C:N ratio. We retained the principal components axes that explained at

least 80% of the variance for both environmental conditions and plant trait data, and these components were subsequently incorporated into the SEM models (Zhang et al., 2024). Environmental conditions were represented by two principal component axes (88.4% variance, Table S2 in the supplements), while plant traits were summarized by three axes (82.7% variance, Table S3 in the supplements). Principal components were computed using singular value decomposition (SVD) via the `prcomp()` function in R, which ensures numerical stability and accurate handling of correlated variables, and all variables were centred and scaled prior to PCA to ensure equal weighting across predictors. Instead, non-metric multidimensional scaling (NMDS) is preferred to reduce dimensionality for compositional data such as species cover because it accommodates non-Euclidean distances, is robust to zero inflation, and better captures ecological dissimilarity patterns (Aerts et al., 2006). Therefore, we applied NMDS using the *vegan* package in R (version 2.6-4). The first two NMDS axes (NMDS1 and NMDS2), which captured the major gradients in species composition, were included in the SEM to represent plant community composition in accordance with Kahmen et al. (2005).

To quantify the effect of guano on vegetation community composition and trait expression we constructed a SEM that excluded the effect of guano, including only environmental conditions as a driver of vegetation characteristics, and compared this null model to the full model that included foliar $\delta^{15}\text{N}$ values as proxy for guano deposition (Figure 3 for the hypothesized relationships). This model included all hypothesized pathways and was refined through backward elimination, removing pathways with $p > 0.05$. Shipley's test of directional separation (D-separation) was employed to ensure that previously omitted significant relationships were included, improving model fit (Shipley, 2009).

Spatial autocorrelation in residuals was addressed using spatial lag models (`lagsarlm` function from the *spatialreg* package, version 1.3-2), with spatial relationships defined by k-nearest neighbor networks ($k = 4$). Residuals were tested for spatial dependence using Moran's I (*spdep* package, version 1.3-1), and spatial adjustments were iteratively applied until no significant autocorrelation remained. Individual pathways were evaluated for normality using the Shapiro-Wilk test on

residuals and assessed for homoscedasticity through residuals versus fitted value plots. All analyses were conducted at the plot
230 level, so transect identity or transect length were not included as model terms.

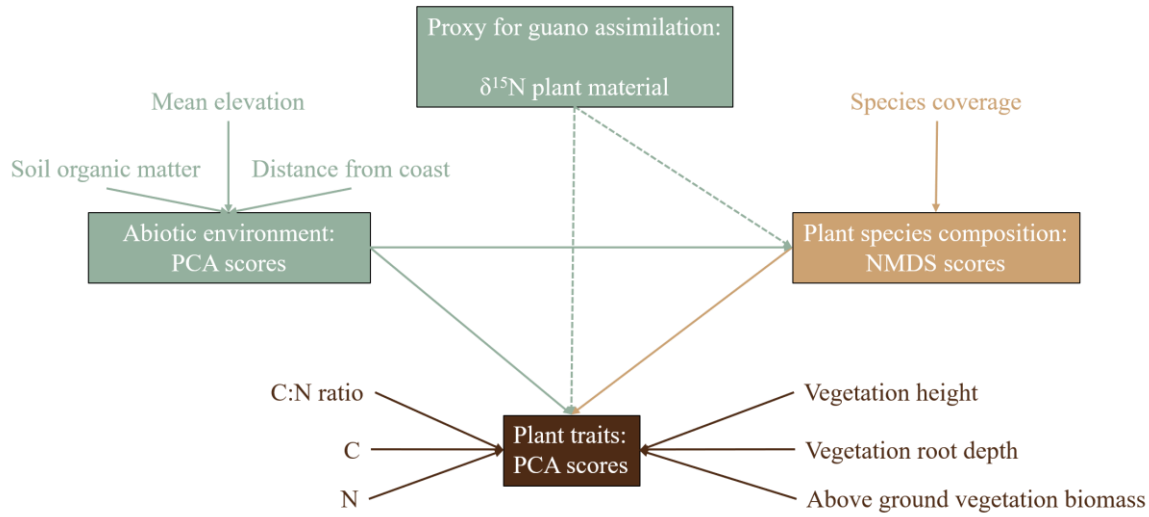


**Figure 3: Design for the SEM in which we hypothesize that environmental conditions, represented by PCA, determine plant species composition, represented by NMDS scores. Both environmental conditions and plant species composition influence plant trait expression. Additionally, guano assimilation, approximated by $\delta^{15}\text{N}$, acts as an isolated environmental factor that directly affects
235 both plant species composition and trait expression.**

2.4 The effect of guano deposition on vegetation-mediated morphological changes

To explore how guano deposition affects island landscape-scale biogeomorphic processes, we used spatial data on the presence of breeding nests to estimate guano deposition, satellite imagery to calculate vegetation productivity indexes and lidar-derived coastal elevation models to explore bed elevation changes.

240 During the 2022 breeding season, bird wardens recorded the location and density of nesting birds following the standardized protocols of the Trilateral Monitoring and Assessment Program (TMAP) (Koffijberg et al., 2017). Counts of breeding pairs were therefore derived from this harmonized monitoring scheme, in which colonial species are surveyed through complete nest or pair counts and widespread breeders are counted within standardized census areas. These data were used to create spatial polygons of nest density per species. Guano deposition was estimated using species-specific faecal excretion rates
245 derived from bird body mass, diet, and metabolic efficiency, based on established allometric equations (Hahn et al., 2007; Karasov, 1990; Nagy et al., 1999), building on the methodology described in Reijers et al., (2024). Bird biomass was determined by linking bird species ID to the global trait database Tobias et al. (2022). Daily excretion rates were multiplied by nest density and the duration of the breeding season to estimate total guano deposition per breeding season (reported as annual totals for comparability across islands).

250 To model the spatial distribution of guano, deposition was assumed to decrease linearly with distance from the nest (Bokhorst et al., 2019; Savage, 2019), up to a maximum of 300 meters (Benkwitt et al., 2021). We refer to this range as the dispersion length throughout this study. A 1-meter resolution Euclidean distance matrix was created around each colony. This matrix was used to generate a distance-decay function, scaling the guano deposition accordingly with its dispersion length. To maintain mass balance, deposition values within colonies were iteratively reduced until the total guano within the colony matched the
255 sum of dispersed deposition in the colony and the surrounding area.

In cases of overlapping colony effects, guano contributions were summed per cell. To evaluate how far guano affects nitrogen assimilation, the model tested dispersion lengths ranging from 1 to 1000 meters. Theoretical deposition was then compared with measured foliar $\delta^{15}\text{N}$ values from the field, and R^2 values were used to determine which spatial scale best predicted nitrogen enrichment. Comparison of modelled guano dispersion with foliar $\delta^{15}\text{N}$ values showed asymptotic improvement
260 beyond ~300 m; thus, 300 m provided the most appropriate and literature-supported fit (R^2 : 0.11, Fig. S6 in the supplements).

2.4.1 Remote sensing of plants and LiDAR for elevation

To study the effects of guano deposition on biogeomorphic interactions, we assessed the impact of guano-induced vegetation changes on sediment bed level dynamics. Vegetation state was represented using the Normalized Difference Vegetation Index (NDVI), calculated from PlanetScope satellite imagery at a 3-meter resolution. The minimum and maximum number of pixels
265 per island were 10979 (Richel) and 501266 (Rottumerplaat) (Table S4 for island specifications). The imagery consisted of orthorectified GeoTIFF files with four spectral bands (near-infrared, red, green, and blue), which compensate for terrain distortions and sensor artifacts to provide Top of Atmosphere (TOA) radiance. NDVI was calculated using the red (R) and near-infrared (NIR) spectra (Tucker, 1979): $NDVI = (NIR - R)/(NIR + R)$.

PlanetScope employs multiple satellites, so to minimize both instrumental and temporal variability, we computed two separate
270 vegetation metrics from different seasonal subsets of the imagery. First, we calculated the mean NDVI from all cloud-free images acquired during the summer months (June–September). This summer mean was used as the representative NDVI value for each year. Second, because the breeding season starts in spring and can influence early vegetation growth, we calculated a Greening Index (GI) based on all NDVI images from the spring period (March–May). GI was defined as the slope of a linear model fitted through the springtime NDVI values, indicating the rate of NDVI change over days. Because overwintering
275 seabird roost mainly on bare island edges, winter guano inputs to vegetated areas are minimal; thus, our guano estimates reflect the breeding-season nutrient pulse.

Elevation data was derived from the LiDAR dataset of the Dutch coast (Rijkswaterstaat, 2017), and converted to a 3-meter resolution raster. Vegetation dynamics were quantified as year-to-year changes in GI and NDVI between 2021 and 2022:

$\Delta GI = GI_{2022} - GI_{2021}$ and $\Delta NDVI = NDVI_{2022} - NDVI_{2021}$ respectively. These were analysed alongside elevation change
280 over the same period: $\Delta Z = Z_{2022} - Z_{2021}$.

2.4.2 Modelling Framework

We modelled sediment bed level change (ΔZ) between 2021 and 2022 across five Wadden Sea islands as a function of
vegetation dynamics, guano deposition, and elevation. Vegetation growth can promote sediment accretion, while its decline
may lead to erosion. These vegetation changes are hypothesized to be influenced by guano fertilization and may vary by island.
285 To test these relationships, we developed two Bayesian spatial models because potentially guano deposition can change the
rate of greening in spring, and/or the resultant biomass after the breeding season in summer. Both models include interaction
terms between guano deposition and vegetation dynamics, and between vegetation dynamics and island identity. They also
account for the initial vegetation state and elevation in 2021:

ΔGI model uses ΔGI to represent the difference in greening rate in spring between 2021 and 2022.

290 **$\Delta NDVI$ model** uses $\Delta NDVI$ to represent changes in vegetation biomass in summer between 2021 and 2022.

To account for spatial autocorrelation in elevation change, we included a spatially structured random field (RF) in both models.
This field was modelled using the Stochastic Partial Differential Equation (SPDE) approach in INLA, which approximates a
Gaussian Random Field through a sparse precision matrix defined by a Matérn covariance function (Bakka et al., 2018; Zuur
and Ieno, 2018). We applied Penalized Complexity (PC) priors to control spatial smoothness: a prior median range of 300 m
295 ($\Pr(\text{range} > 300 \text{ m}) = 0.5$), corresponding to the size of the smallest island (Richel), and a PC prior on the marginal standard
deviation ($\Pr(\sigma > 1) = 0.1$), allowing sufficient flexibility while regularizing spatial variation.

The model structures are:

Model 1:

$$\Delta Z = \beta_1 \text{Guano} \times \Delta GI + \beta_2 GI_{2021} + \beta_3 Z_{2021} + \beta_4 \text{island} \times \Delta GI + RF$$

300 **Model 2:**

$$\Delta Z = \beta_1 \text{Guano} \times \Delta NDVI + \beta_2 NDVI_{2021} + \beta_3 Z_{2021} + \beta_4 \text{island} \times \Delta NDVI + RF$$

We then subsampled up to 1000 vegetated cells per island to balance spatial coverage and computational load. Cells were
classified as vegetated if $NDVI > 0.2$, following Reijers et al. (2024). Guano deposition was log-transformed as $\log(\text{Guano} +$
 $1)$ to reduce the influence of extreme values. All continuous variables were standardised by subtracting the mean and dividing
305 by the standard deviation.

A triangular mesh was created for each island to define the spatial domain, with a maximum edge length of 30 m within islands
and up to 3000 m between islands. The mesh boundary followed the MHT line of the islands. Models were fitted in R using
the INLA package, which provided estimates for main effects, posterior spatial fields, and model diagnostics (DIC and WAIC).
Residuals were evaluated for normality, homoscedasticity, and spatial structure. Key covariates and interaction terms were
310 visualized against residuals to validate model assumptions. In addition to standard diagnostics, we evaluated model robustness
using Bayesian checks appropriate for INLA, including sensitivity to spatial prior specification and mesh resolution, and

posterior predictive checks comparing observed ΔZ with model predictions (see model validation, Fig. S12-14 in the Supplements).

3 Results

315 3.1 The effect of guano deposition on species composition and plant traits

3.1.1 Reduced dimensionality of environmental variables, plant species composition, and plant traits

To evaluate how environmental conditions influence vegetation traits and composition, we constructed a piecewise structural equation model (SEM) (Figure 5). Higher values on $PC1_{\text{environment}}$ represent inland sites with higher organic matter content. $PC2_{\text{environment}}$ increases toward lower-elevation sites (Figure 4a, and Table S2 in the supplements). PCA scores related to plant
320 traits are displayed in Figure 4c-d; loadings can be found in Table S3 in the supplements. Higher $PC1_{\text{plant trait}}$ scores reflect lower vegetation height, biomass, root depth and foliar carbon. $PC2_{\text{plant trait}}$ increases with higher nitrogen content and lower C:N ratio. $PC3_{\text{plant trait}}$ captures a trade-off between rooting depth and aboveground height: higher $PC3_{\text{plant trait}}$ scores indicate shallow-rooted but taller plant.

Species composition was ordinated using NMDS (stress = 0.13). Higher NMDS1 values indicate communities dominated by
325 sand-preferring species, while lower values reflect mud-preferring species (Figure 4b). Along NMDS2, shifts depend on substrate origin: on sand, increasing values correspond to grasses like *Ammophila arenaria*, while decreasing values reflect more forbs such as *Atriplex littoralis*. In muddy environments, increasing NMDS2 values indicate a shift toward pioneer species such as *Salicornia procumbens*, while decreasing values reflect a transition toward climax species like *Elytrigia atherica*.

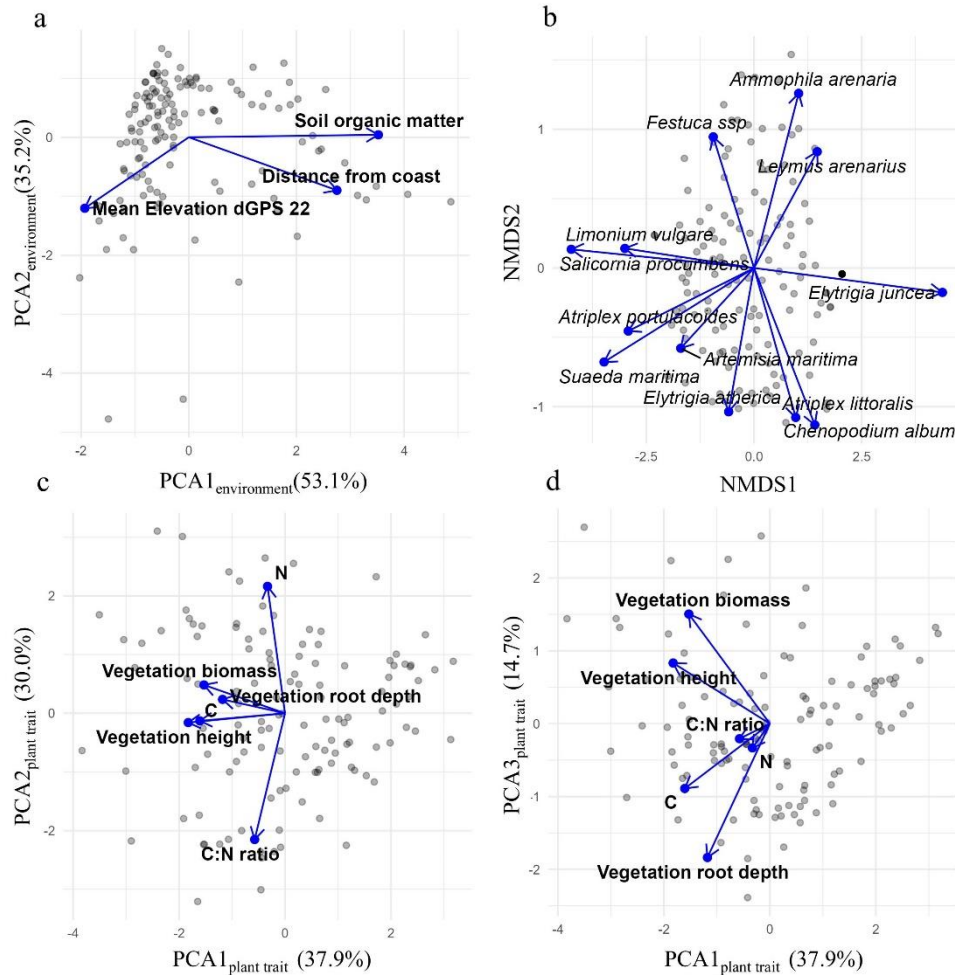


Figure 4: PCA and NMDS bi-plots of (a) environmental variables, (b) plant species composition, and (c-d) plant traits. The NMDS plot displays the 12 most abundant species.

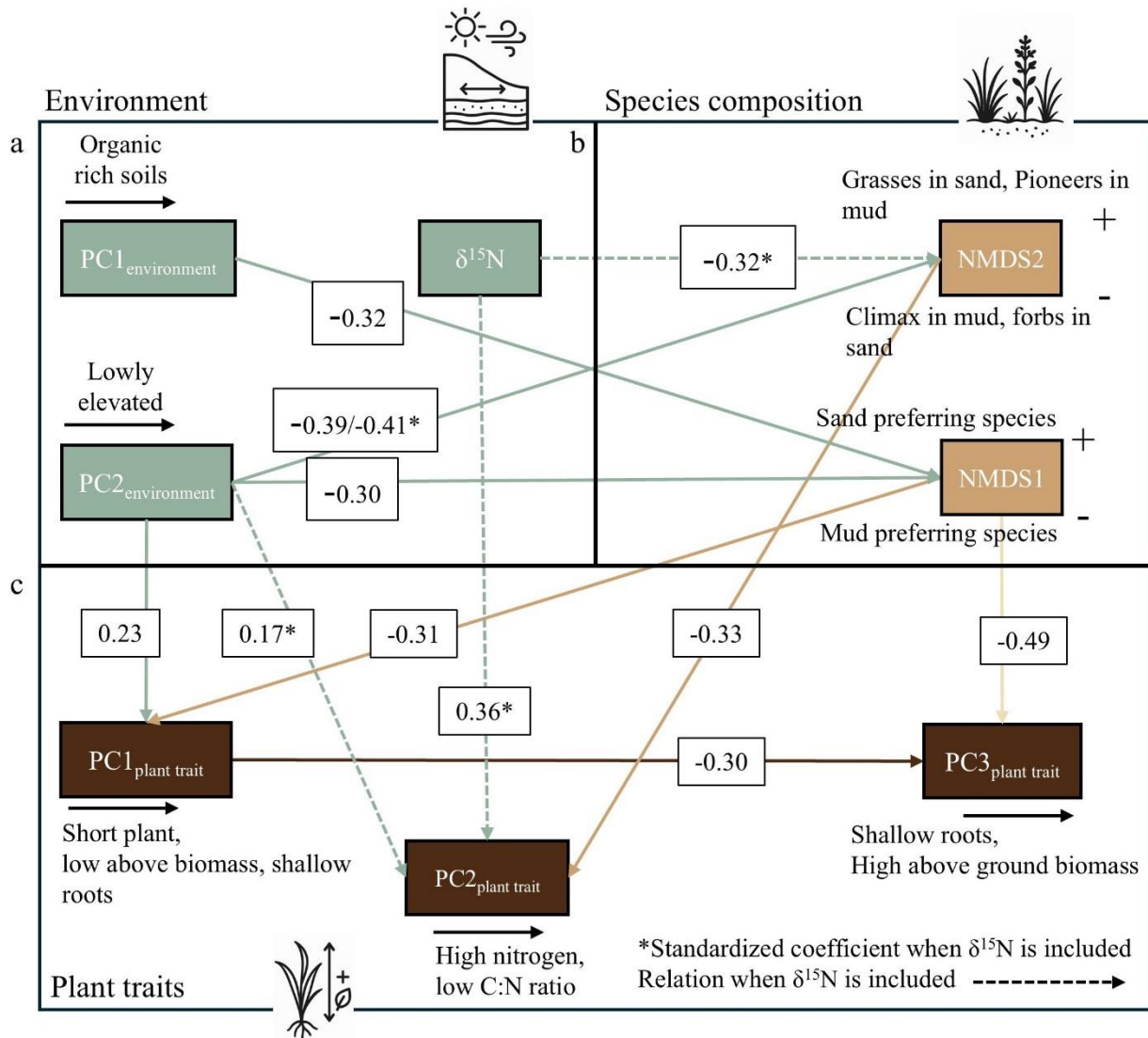
3.1.2 The (in)direct effects on environmental conditions on vegetation composition and trait expression

335 In the model without $\delta^{15}\text{N}$, organic-rich soils are associated with mud-preferring species ($\text{PC1}_{\text{environment}} \rightarrow \text{NMDS1}: -0.32$), and lower elevations also shift composition toward mud-preferring communities ($\text{PC2}_{\text{environment}}$ of environment $\rightarrow \text{NMDS1}: -0.30$), (Figure 5b). These compositional shifts affect trait expression: sand-preferring species generally have higher biomass and deeper roots ($\text{NMDS1} \rightarrow \text{PC1}_{\text{plant trait}}: -0.31$), while forbs on sand or climax species on mud have higher nitrogen and lower C:N ratios ($\text{NMDS2} \rightarrow \text{PC2}_{\text{plant trait}}: -0.33$), (Figure 5c). Elevation directly promotes traits linked to higher biomass and deeper roots ($\text{PC2}_{\text{environment}} \rightarrow \text{PCA1}$ of plant traits: 0.23). This indicates that within the same species composition, these traits can be

340

altered by elevation differences. The model without $\delta^{15}\text{N}$ explains 67% of NMDS1, 21% of NMDS2 and 44% of PC1_{plant trait}, 20% of PC2_{plant trait} and 27% of PC3_{plant trait}, which changes upon the inclusion of $\delta^{15}\text{N}$.

When we include $\delta^{15}\text{N}$, the model explains 9% more variance in plant species composition (NMDS2), and 5% more variance in plant traits (PC2_{plant trait}). Although increases in R^2 alone can arise from adding predictors, the ecological relevance of guano assimilation is supported by the significant and directionally consistent paths in the SEM: guano assimilation shifts composition toward climax in mud or forb-dominated communities in sand ($\delta^{15}\text{N} \rightarrow \text{NMDS2}$: -0.32) and increases foliar nitrogen content independent of species composition ($\delta^{15}\text{N} \rightarrow \text{PC2}_{\text{plant trait}}$: 0.36), (Figure 5c and Fig. S5 in the supplements). Because NMDS2 feeds into PC2_{plant trait}, $\delta^{15}\text{N}$ also indirectly influences plant trait through changing the plant species composition. Additionally, a new path emerges in which lower elevation is associated with lower nitrogen concentrations (PC2_{environment} \rightarrow PC2_{plant trait}: 0.17). The latter compensates for the fact that higher foliar $\delta^{15}\text{N}$ is associated with higher N; this effect is reduced in low-lying areas like salt marshes, likely because $\delta^{15}\text{N}$ is less assimilated by salt marsh species, because of the abundance of organic matter (Fig. S5 in the Supplements).



355 **Figure 5: Piecewise SEM of (a) environmental PCA scores, (b) species-composition NMDS axes, and (c) plant-trait PCA scores.** Arrows show significant pathways with standardized coefficients; an asterisk (*) marks coefficients from the $\delta^{15}N$ -inclusive model ($\delta^{15}N$ as guano proxy), and dashed arrows are new $\delta^{15}N$ -driven paths. Goodness-of-fit statistics of the model without $\delta^{15}N$ indicate adequate model performance ($\chi^2 = 14.86$, $p = 0.25$; Fisher's $C = 30.62$, $p = 0.17$; AIC = 1478). Upon the inclusion of $\delta^{15}N$, the updated model displays an improved fit ($\chi^2 = 20.15$, $p = 0.17$; Fisher's $C = 40.21$, $p = 0.10$; AIC = 1459).

3.2 The effect of guano deposition on vegetation-mediated morphological changes

360 3.2.1 Vegetation state changes by guano deposition, affecting morphological changes

Two Bayesian hierarchical modelling approaches enabled us to analyse how the timing of vegetation development and fertilization by guano affect sediment trapping through shifts in vegetation state (Figure 6, and Table S7, Fig. S9 and Fig. S10

in the Supplements). This effect is analysed through the interaction between guano, changes in vegetation state and change in sediment bed level. We found that the interaction between guano and vegetation development differed notably between models. In the ΔGI model, the interaction between guano and ΔGI on the z-standardized scale was slightly positive: 0.010 (95% credible interval (95% CI): 0.000 to 0.021). This indicates that guano fertilization enhances the ability of spring vegetation greening to promote sedimentation, in line with the hypothesis (Figure 6). Surprisingly, the $\Delta NDVI$ model, the interaction between guano and $\Delta NDVI$ was slightly negative: -0.033 (95% CI: -0.053 to -0.013) on the z-standardized scale (Figure 6). This means that positive bird-induced sediment bed level change is expected at locations that are high in guano deposition, and negative in $\Delta NDVI$.

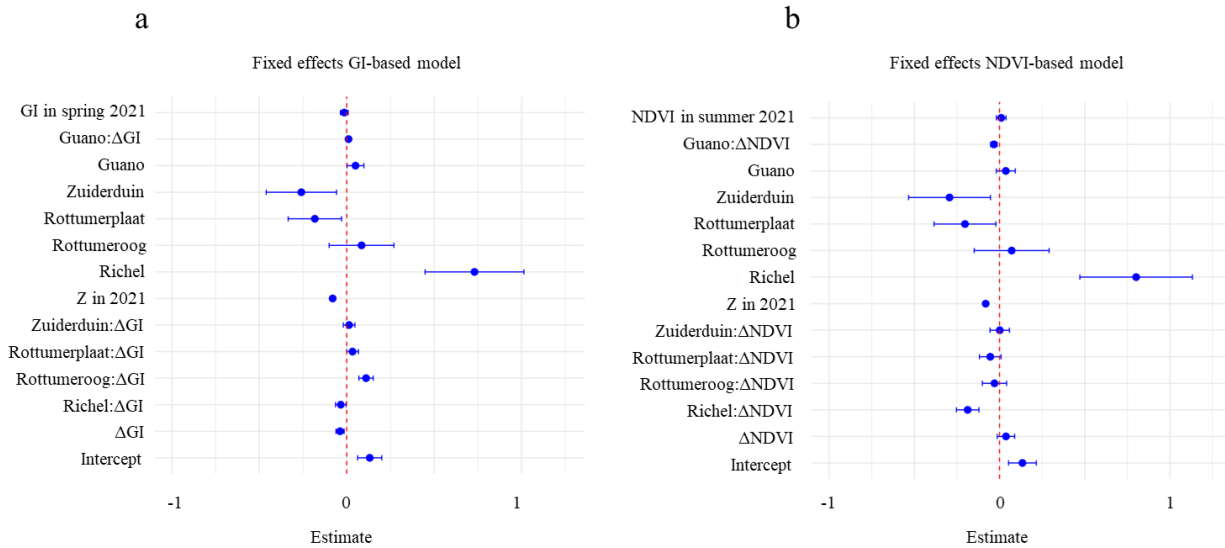
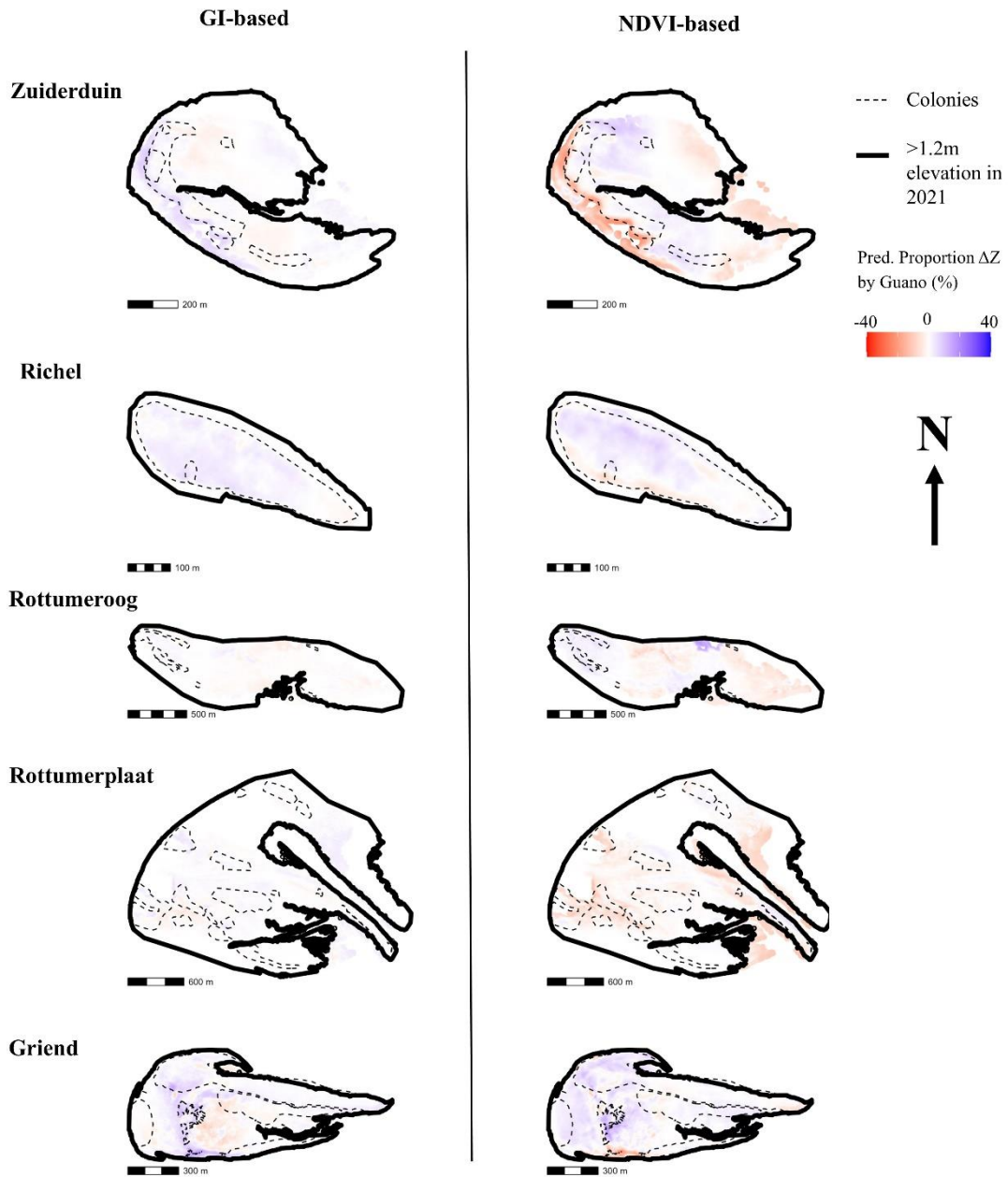


Figure 6: Main-effect estimates (markers) with 95% credible intervals for (a) GI-based and (b) NDVI-based spatial models. All continuous predictors were z-standardised prior to modelling; coefficients therefore represent the effect of a one-standard-deviation change in each predictor. Scaling factors can be found in Table S8. The GI model's spatial range (175 m) is shorter than the NDVI model's (206 m), and both have similar random-field SD (~0.3 m). Model DIC/WAIC are comparable (GI: -2203/-2295; NDVI: -2228/-2290). Spatial maps of ΔGI , $\Delta NDVI$ and ΔZ are in Supplement Fig. S11.

3.2.2 The importance of the guano-induced changes in sediment bed level change varies spatially

The impact of guano deposition on an island's morphology depends on the relative influence of other factors shaping sediment dynamics. The spatially explicit percentual contribution to elevation change is depicted in Figure 7. On islands like Rottumeroog and Rottumerplaat, where guano deposition is low and vegetation remains stable, but morphological change is significant, our models attribute this variation primarily to island-specific effects or the spatial random field. Conversely, on islands where guano deposition is high but the inherent depositional trend is weak, guano-driven sedimentation plays a more prominent role, as observed on the south of Griend and west of Zuiderduin, where sedimentation is explained up to 13% by

interactions between guano and vegetation (NDVI-based 99th-percentile of the predicted proportion ΔZ by guano). In contrast,
385 Richel also experiences high guano deposition, but its naturally high sedimentation rates dominate morphological change,
reducing the relative contribution of guano in shaping its landscape.



390 **Figure 7: Predicted proportion (%) of change in elevation imposed by an interaction effect between the change in vegetation state (GI or NDVI) and guano deposition with respect to the absolute value of all modelled terms. The interaction term can become negative, depending on the sign of the vegetation state change. The predicted proportion of change in elevation, can therefore, also be negative. Negative means erosion, positive is erosion with respect to the absolute values of all terms of the prediction. The thick black lines indicate the edge of the island, the MHT line. The thin black lines indicates the location of the colonies.**

Guano deposition, without interaction with Δ GI or Δ NDVI, had a positive effect on changes in sediment bed level in both models (Figure 6). From an ecological perspective, this can be viewed as a positive association between breeding bird densities and locations where less erosion occurs. In the Δ GI model, guano deposition had an effect of 0.050 (95% CI: 0.002 to 0.098) on changes in sediment bed level. In the Δ NDVI model, the effect was slightly lower and uncertain (0.037 (95% CI: -0.019 to 400 0.092)), suggesting a weaker direct relationship between guano and morphological change when approximating vegetation through Δ NDVI.

3.2.4 Abiotic and island-specific contributions to sediment dynamics

While the direct effects of guano deposition on sediment bed level change are central to this study, both models show that other factors also play a role. Initial elevation in 2021 was a strong negative predictor of sediment bed level change (GI-based: 405 -0.080 (95% CI: -0.095 to -0.066); NDVI-based: -0.081 (95% CI: -0.096 to -0.067), indicating that higher areas experienced more erosion or less accretion in the years we analysed. Island identity also significantly influenced geomorphic responses: Richel showed more accretion (GI-based: 0.731 (95% CI: 0.448 to 1.015); NDVI-based: 0.802 (95% CI: 0.474 to 1.136)), while Rottumerplaat and Zuiderduin showed more erosion compared to Griend. Interestingly, several islands exhibited negative interactions between vegetation change and sedimentation, particularly Richel (GI-based: -0.034 (95% CI: -0.064 to 410 -0.004); NDVI-based: -0.187 (95% CI: -0.253 to -0.121)), where vegetation decline may reflect rapid burial due to strong sedimentation.

4 Discussion

Our study demonstrates that seabird guano is a biotic driver modulating vegetation dynamics and, in turn, biogeomorphic interactions. While classic environmental filters such as elevation and soil organic matter remain primary determinants of vegetation composition and functional trait expression, guano shifts plant communities toward more nitrophilous, high-productivity species and increases foliar nitrogen, as shown by our structural equation models (Figure 5). However, we found no consistent evidence that guano alters above- or belowground traits typically associated with sediment stabilization. At the landscape scale, elevation was the dominant predictor of elevation change, with higher areas experiencing more erosion or less accretion in the years we analysed. Guano- or vegetation-mediated effects on elevation were generally weak, except in localized areas where their interaction explained up to 13% of variation in sediment dynamics. This spatial heterogeneity was also reflected in island-specific patterns: at Rottumeroog, early-season greening had a strong positive effect on sediment accretion, whereas at Richel, high background sedimentation appeared to mask the influence of vegetation. Together, these findings suggest that while guano influences vegetation composition and traits related to nitrogen assimilation, its role in modulating vegetation–landform feedbacks is highly context-dependent. Integrating trait data from the field with landscape-scale remote sensing thus provides a powerful approach to unravel the complex, spatially variable effects of biotic nutrient inputs on coastal landscape development (Cavender-bares et al., 2022; Lausch et al., 2018).

4.1 Guano can change local vegetation characteristics

Our findings demonstrate that guano can drive shifts in plant species composition, which, in turn, affects trait expression. The inclusion of $\delta^{15}\text{N}$ in our structural equation models revealed an improved explanatory power, explaining 9% more variance in plant species composition and 5% more variance in plant traits, accentuating that guano overrides or modifies abiotic constraints (Figure 5). These results support the conceptual framework of bottom-up, nutrient-driven succession in coastal systems (Olf et al., 1993). Specifically, nutrient-rich guano promotes the proliferation of nitrophilous, later-successional species on both sand (e.g., *Atriplex littoralis*) and mud (e.g., *Elytrigia atherica*), independent of background community structure. This is in correspondence with earlier studies on *Atriplex ssp.* on seabird islands (Anderson and Polis, 1999). Yet, plants in nutrient-deprived sandy soils appear to be more reliant on guano subsidies, as we observed that primarily sand-preferring communities displayed foliar $\delta^{15}\text{N}$ enrichment, suggesting elevated nitrogen assimilation from guano (Fig. S5 in the Supplementary Material). These fertilization effects are further reflected in elevated foliar nitrogen and reduced C:N ratios, particularly in forb-dominated or climax communities, comparable with earlier observations (McKane et al., 1990; Reijers et al., 2024; Wainright et al., 1998). Sand-preferring species also exhibit traits linked to resource acquisition, such as greater biomass and deeper rooting. Root growth is generally enhanced in nitrogen-limited soils (Ericsson, 1995), such as sand, in comparison to mud. In this context, sand nourishment may further influence vegetation through both functional and compositional pathways by altering sediment characteristics and nutrient availability. Although the nutrient content of the nourished sand at Griend is not known, any direct nourishment-related nutrient signal was likely weak during our study, which

445 was conducted approximately six years after nourishment. Evidence from comparable coastal systems suggests that sediment
nutrient levels tend to converge toward background conditions within several years following nourishment (Pit et al., 2020).
Additionally, we do not expect strong year-round effects of guano, as winter roosting birds defecate mainly along the island
edges where little vegetation grows, and most guano nitrogen is rapidly lost through leaching, volatilisation, and runoff (Loder
III et al., 1996; Otero et al., 2018; Peña-Lastra et al., 2022; Riddick et al., 2012); only a small fraction may persist in slowly
450 decomposing plant material and influence early spring growth (Kooijman and Besse, 2002).

Additionally, even within a given species composition, plants show substantial trait plasticity in response to elevation (Schulte
Ostermann et al., 2021). In lower-lying sites, characterised by more saline or frequently inundated conditions, plants tend to
develop shallower roots, lower biomass, and reduced vegetation height, potentially as adaptive strategies to cope with
455 environmental stress (De Battisti et al., 2020). However, despite clear evidence that guano influences species composition and
nutrient assimilation, we did not find a consistent link between guano enrichment and the modification of biogeomorphological
traits like above-ground biomass, vegetation height, or rooting depth. This finding is partly in agreement with Reijers et al.
(2024), who also observed guano-induced nitrogen assimilation. However, unlike our results, they identified a quadratic
relationship between guano enrichment and the aboveground biomass of vegetation. This suggests that while guano enhances
460 nutrient dynamics and supports succession, its contribution to feedbacks between vegetation and landscape formation remains
less certain under the studied conditions. One explanation may lie in the seasonal dynamics of trait expression: traits like
biomass and height may temporarily increase due to spring nutrient uptake, enhancing sediment trapping (Zarnetske et al.,
2012). However, this process may also reduce relative vegetation height as sediment accumulates (Derijckere et al., 2023).
Since our measurements were taken in summer, the timing may have obscured any guano-related enhancement of
465 biogeomorphic traits. Additionally, our approach of reducing dimensionality of plant traits, might also have limited us to reveal
the non-linear relationship between guano enrichment and bio geomorphic plant traits found in Reijers et al. (2024).

4.2 Guano as driver for landscape modification

Our remote sensing analysis confirms that seabird guano plays a significant role in shaping biogeomorphic dynamics across
sandy islands in the Wadden Sea, particularly by enhancing sediment deposition in fertilised vegetated areas. We found that
470 the interaction between guano and vegetation development differed depending on how the vegetation state change was
measured. When vegetation dynamics were captured through early-season greening (ΔGI), guano amplified the positive effects
of vegetation on sedimentation, indicating synergistic effects between fertilization and spring productivity. This suggests an
earlier activation of biogeomorphic capabilities in plants when fertilised with guano (Figure 8). This supports the idea that
plant ecosystem engineering is context-dependent and influenced by the timing and age-related expression of functional traits
475 (van de Ven et al., 2023). A summer-season decline in vegetation cover compared to the previous year, particularly under
guano-rich conditions, is associated with subsequent sediment burial (Figure 8). Notably, this pattern aligns with the observed
spatial distribution of sedimentation on the western coast of Zuiderduin (Figure 7).

At this location, a sandy barrier, home to a dense cormorant colony and exposed to high rates of guano deposition, has accreted substantially. Due to rapid sediment burial, both NDVI values declined, reflecting a reduction in vegetation state in summer. The demise of vegetation cover is known to reflect sediment burial (Miller et al., 2010). However, both sediment trapping capacity and resilience to burial are closely tied to the vertical growth potential of biogeomorphic dune grasses (Strypsteen et al., 2024). While vegetation density may have decreased due to burial, it is possible that vertical growth was enhanced by guano fertilization, enabling the plants to maintain their role in sediment capture. Across the landscape, guano–vegetation interactions contributed modest amounts to modelled sediment bed-level change (~1–3% on average), but stronger effects occurred close to seabird colonies, reaching ~6% in the GI-based model and ~13% in the NDVI-based model (99th-percentile of the predicted proportion ΔZ by guano). These localised peaks are obscured when averaging across entire islands (Figure 7).

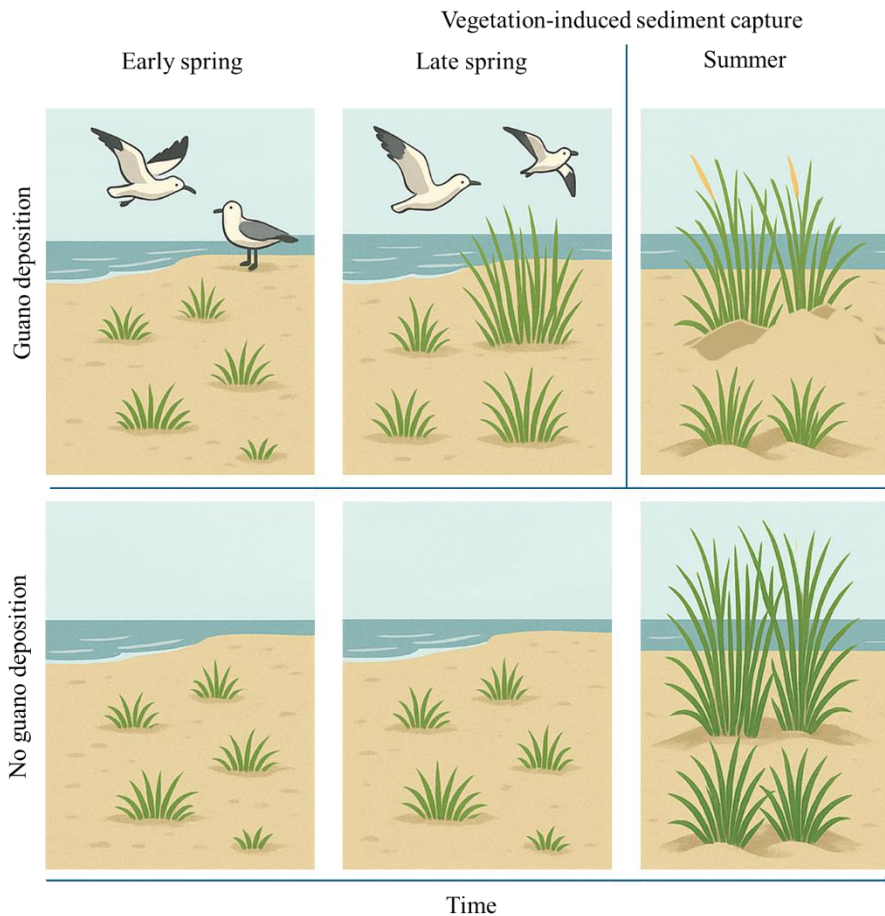


Figure 8: This illustration compares vegetation development with and without guano deposition over time. In early spring (left column), guano input by seabirds initiates fertilization, enhancing plant growth. By spring (middle column), this leads to increased vegetation height and biomass, strengthening the plants' ability to trap sediment (biogeomorphic feedback). In summer (right column), this feedback is visible through dune formation in guano-enriched areas. However, the apparent vegetation height

decreases slightly as plants become partially buried by sediment. In contrast, areas without guano show less growth and weaker biogeomorphic effects throughout the season.

4.3 Mechanistic understanding and causality

495 This research contributes to the growing body of literature showing that allochthonous nutrient inputs, such as seabird guano, can influence plant species composition and functional traits (Ellis, 2005; Maron et al., 2006; Reijers et al., 2024). Crucially, we provide novel evidence that these bird-derived nutrient subsidies not only reshape vegetation dynamics but also drive landscape evolution, enhancing sediment deposition and coastal morphodynamics via strengthened vegetation–sediment feedbacks. Biophysical feedback mechanisms are well-documented in other coastal systems such as dunes (Bonte et al., 2021),
500 salt marshes (Allen, 2000), seagrass beds (Forsberg et al., 2018), and mangroves (van Maanen et al., 2015). Causality, however, remains difficult to establish. While our results show a positive association between guano deposition, vegetation dynamics, and sediment accumulation, these patterns could also reflect seabird preferences for nesting in areas that already have favorable conditions, such as stable, vegetated sites with higher sedimentation and less erosion (DeRose-Wilson et al., 2013; Raynor et al., 2012), where eggs are less likely to be washed away (Bailey et al., 2017; van de Pol et al., 2024). It
505 is likely that both processes, vegetation-induced sedimentation and seabird habitat selection, are simultaneously at play, suggesting the role of birds as agents of their own habitat formation. To disentangle these reciprocal relationships and better understand causality, manipulative experiments are needed that vary guano deposition rates and plant species identity to test how guano affects plant trait plasticity and sedimentation feedbacks. Yet, because these feedbacks unfold across spatial and temporal scales that are challenging to capture through fieldwork alone, empirical data must be integrated into trait-based
510 ecological frameworks and dynamic numerical models. Currently, such models rarely incorporate plant traits, limiting their ability to simulate guano-driven geomorphological change. Advancing these modelling tools is critical, not only to improve our understanding of biogeomorphic processes but also to inform conservation strategies. As coastal ecosystems face growing threats from sea-level rise (van de Pol et al., 2024) and coastal squeeze (Lansu et al., 2024), technical progress is needed to predict how guano-mediated changes in vegetation influence landscape development and, in turn, seabird habitat availability
515 (Paleczny et al., 2015). These insights are directly relevant for current seabird restoration practices. Seabird restoration efforts, such as acoustic luring, decoys, or nest translocation, are increasingly used to re-establish colonies on coastal islands (Jones et al., 2025; Jones and Kress, 2012; Spatz et al., 2023). Our results show that such interventions will not only affect bird populations but also transform plant communities through guano enrichment, with consequences for sediment accretion and island resilience. Effective restoration therefore requires a holistic approach that anticipates these vegetation shifts. Supporting
520 nitrophilous, sediment-accreting plant species before or alongside seabird return can help ensure that nutrient inputs strengthen, rather than weaken, the stability of restored islands.

5 Conclusions

In conclusion, our spatially explicit study combines fine-scale field measurements of plant traits with landscape-scale remote sensing (NDVI and coastal elevation differencing) to provide the first quantitative evidence that seabird guano inputs modulate
525 vegetation–sedimentation feedbacks and drive coastal landscape evolution. Structural equation models and Bayesian hierarchical remote-sensing analyses reveal that these guano effects on species composition, foliar nitrogen content, and sediment deposition are highly context-dependent, varying with elevation, substrate type, season, and island-specific conditions, nuances often overlooked in whole-island studies. Mechanistically, while high guano levels are associated with nitrophilous, high-productivity species and boosts foliar nitrogen, its impact on biogeomorphic traits such as biomass, rooting
530 depth, and vegetation height exhibits pronounced spatial and seasonal variability. Our integrated approach, combining in situ trait measurements, structural equation modelling, remote sensing analyses, and Bayesian spatial modelling, provides a useful framework for exploring nutrient–vegetation–geomorphology interactions in other soft-sediment ecosystems.

Data availability. Upon acceptance, the data supporting our results will be freely available and the data DOI will be included.
535

Author contributions. FFR, LLG, CJC, GR and VCR conceptualized the study. FFR, MPAZ, CT collected all field data. CT and FFR performed all lab analyses. PG and FFR performed the remote sensing analysis. FFR performed all data analyses and wrote the original draft. VCR, CJC and LLG secured the funding. All authors reviewed on the original draft.

540 *Competing interests.* The contact author has declared that none of the authors has any competing interests.

Acknowledgements. We thank Ane Derk van Rees, Nadia Hijner, Solveig Hofer, Paul Berghuis, and Eva Lansu for their invaluable assistance during fieldwork. We are grateful to Wim-Jan Boon and all employees of the Waddenunit for their support with transport to the islands and technical assistance, particularly Jan Kostwinner, Arjen Dijkstra, and Romke
545 Kleefstra. We thank Richard Deen and Anne Dekkinga for their support for acquiring the permits for the fieldwork sites. For providing bird data and local ecological insights, we thank Jaap Kloosterhuis, Jan Veen, Erik Jansen, Allix Brenninkmeijer, Thea Smit, Marc van der Aa, Erwin Goutbeek, and Carl Zuhorn, and Kees Koffijberg. Marcel van der Meer and Ronald van Bommel are acknowledged for their academic and technical support for stable isotope analysis

550 *Financial support.* This work is part of the avian-nutrient pump project funded by a UU-NIOZ collaborative grant awarded to VCR and CJC. VCR was additionally supported by NWO-Veni grant VI.Veni.212.059.

6 References

Aerts, R., Van Overtveld, K., Haile, M., Hermy, M., Deckers, J., and Muys, B.: Species composition and diversity of small

- 555 Afromontane forest fragments in northern Ethiopia, *Plant Ecol.*, 187, 127–142, <https://doi.org/10.1007/s11258-006-9137-0>, 2006.
- Allen, J. R. L.: Morphodynamics of Holocene salt marshes: A review sketch from the Atlantic and Southern North Sea coasts of Europe, *Quat. Sci. Rev.*, 19, 1155–1231, [https://doi.org/10.1016/S0277-3791\(99\)00034-7](https://doi.org/10.1016/S0277-3791(99)00034-7), 2000.
- Anderson, W. B. and Polis, G. A.: Nutrient Fluxes from water to land: seabirds affect plant nutrient status on Gulf of California islands, *Oecologia*, 118, 324–332, 1999.
- 560 Anderson, W. B., Wait, D. A., and Stapp, P.: Resources from another place and time: Responses to pulses in a spatially subsidized system, *Ecology*, 89, 660–670, <https://doi.org/10.1890/07-0234.1>, 2008.
- Appoo, J. and Bunbury, N.: Seabird nutrient subsidies enrich mangrove ecosystems and are exported to nearby coastal habitats, *iScience*, 27, 109404, <https://doi.org/10.1016/j.isci.2024.109404>, 2024.
- 565 Bailey, L. D., Ens, B. J., Both, C., Heg, D., Oosterbeek, K., and van De Pol, M.: No phenotypic plasticity in nest-site selection in response to extreme flooding events, *Philos. Trans. R. Soc. B Biol. Sci.*, 372, 20160139, <https://doi.org/10.1098/rstb.2016.0139>, 2017.
- Bakka, H., Rue, H., Fuglstad, G. A., Riebler, A., Bolin, D., Illian, J., Krainski, E., Simpson, D., and Lindgren, F.: Spatial modeling with R-INLA: A review, *Wiley Interdiscip. Rev. Comput. Stat.*, 10, 1–24, <https://doi.org/10.1002/wics.1443>, 2018.
- 570 Bakker, J. P., Berg, M. P., Grootjans, A. P., Olf, H., Schrama, M., and Reijers, V. C.: Biogeomorphological aspects of a model barrier island and its surroundings - Interactions between abiotic conditions and biota shaping the tidal and terrestrial landscape : A synthesis, *Ocean Coast. Manag.*, 239, 106624, <https://doi.org/10.1016/j.ocecoaman.2023.106624>, 2023.
- Barrett, K., Anderson, W. B., Wait, D. A., Grismer, L. L., Polis, G. A., and Rose, M. D.: Marine subsidies alter the diet and abundance of insular and coastal lizard populations, *Oikos*, 109, 145–153, <https://doi.org/10.1111/j.0030-1299.2005.13728.x>,
- 575 2005.
- De Battisti, D., Fowler, M. S., Jenkins, S. R., Skov, M. W., Rossi, M., Bouma, T. J., Neyland, P. J., and Griffin, J. N.: Intraspecific root trait variability along environmental gradients affects salt marsh resistance to lateral erosion, *Front. Ecol. Evol.*, 7, 1–11, <https://doi.org/10.3389/fevo.2019.00150>, 2019.
- De Battisti, D., Fowler, M. S., Jenkins, S. R., Skov, M. W., Bouma, T. J., Neyland, P. J., and Griffin, J. N.: Multiple trait dimensions mediate stress gradient effects on plant biomass allocation, with implications for coastal ecosystem services, *J. Ecol.*, 108, 1227–1240, <https://doi.org/10.1111/1365-2745.13393>, 2020.
- 580 Bauer, S. and Hoyer, B. J.: Migratory animals couple biodiversity and ecosystem functioning worldwide, *Science (80-.)*, 344, <https://doi.org/10.1126/science.1242552>, 2014.
- Benkwitt, C. E., Gunn, R. L., Le Corre, M., Carr, P., and Graham, N. A. J.: Rat eradication restores nutrient subsidies from seabirds across terrestrial and marine ecosystems, *Curr. Biol.*, 31, 2704–2711.e4, <https://doi.org/10.1016/j.cub.2021.03.104>, 2021.
- Boere, G. C. and Piersma, T.: Flyway protection and the predicament of our migrant birds: A critical look at international conservation policies and the Dutch Wadden Sea, *Ocean Coast. Manag.*, 68, 157–168,

- <https://doi.org/10.1016/j.ocecoaman.2012.05.019>, 2012.
- 590 Bokhorst, S., Convey, P., and Aerts, R.: Nitrogen inputs by marine vertebrates drive abundance and richness in Antarctic terrestrial ecosystems., *Curr. Biol.*, 29, 1721–1727, 2019.
- Bonte, D., Batsleer, F., Provoost, S., Reijers, V., Vandegehuchte, M. L., Van De Walle, R., Dan, S., Matheve, H., Rauwoens, P., Strypsteen, G., Suzuki, T., Verwaest, T., and Hillaert, J.: Biomorphogenic Feedbacks and the Spatial Organization of a Dominant Grass Steer Dune Development, *Front. Ecol. Evol.*, 9, 1–12, <https://doi.org/10.3389/fevo.2021.761336>, 2021.
- 595 Van Boxel, J. H., Arens, S. M., and Van Dijk, P. M.: Aeolian processes across transverse dunes. I: Modelling the air flow, *Earth Surf. Process. Landforms*, 24, 255–270, [https://doi.org/10.1002/\(sici\)1096-9837\(199903\)24:3<255::aid-esp962>3.0.co;2-3](https://doi.org/10.1002/(sici)1096-9837(199903)24:3<255::aid-esp962>3.0.co;2-3), 1999.
- Buelow, C. A., Baker, R., Reside, A. E., and Sheaves, M.: Nutrient subsidy indicators predict the presence of an avian mobile-link species, *Ecol. Indic.*, 89, 507–515, <https://doi.org/10.1016/j.ecolind.2018.02.029>, 2018.
- 600 Cavender-bares, J., Schneider, F. D., Santos, M. J., Armstrong, A., Carnaval, A., Dahlin, K. M., Fatoyinbo, L., Hurtt, G. C., Schimel, D., Townsend, P. A., Ustin, S. L., Wang, Z., and Wilson, A. M.: Integrating remote sensing with ecology and evolution to advance biodiversity conservation, *Nat. Ecol. Evol.*, 6, 506–519, <https://doi.org/10.1038/s41559-022-01702-5>, 2022.
- Compton, T. J., Holthuijsen, S., Koolhaas, A., Dekinga, A., ten Horn, J., Smith, J., Galama, Y., Brugge, M., van der Wal, D., 605 van der Meer, J., van der Veer, H. W., and Piersma, T.: Distinctly variable mudscapes: Distribution gradients of intertidal macrofauna across the Dutch Wadden Sea, *J. Sea Res.*, 82, 103–116, <https://doi.org/10.1016/j.seares.2013.02.002>, 2013.
- Corenblit, D., Baas, A. C. W., Bornette, G., Darrozes, J., Delmotte, S., Francis, R. A., Gurnell, A. M., Julien, F., Naiman, R. J., and Steiger, J.: Feedbacks between geomorphology and biota controlling Earth surface processes and landforms: A review of foundation concepts and current understandings, *Earth-Science Rev.*, 106, 307–331, 610 <https://doi.org/10.1016/j.earscirev.2011.03.002>, 2011.
- Derijkere, J., Strypsteen, G., and Rauwoens, P.: Early-stage development of an artificial dune with varying plant density and distribution, *Geomorphology*, 437, 108806, <https://doi.org/10.1016/j.geomorph.2023.108806>, 2023.
- DeRose-Wilson, A., Fraser, J. D., Karpanty, S. M., and Catlin, D. H.: Nest-site selection and demography of Wilson’s Plovers on a North Carolina barrier island., *J. F. Ornithol.*, 84, 329–344, 2013.
- 615 Dickey, J., Wengrove, M., Cohn, N., Ruggiero, P., and Hacker, S. D.: Observations and modeling of shear stress reduction and sediment flux within sparse dune grass canopies on managed coastal dunes, *Earth Surf. Process. Landforms*, 48, 907–922, <https://doi.org/10.1002/esp.5526>, 2023.
- Dunn, R. E., Carr, P., Benkwitt, C. E., Graham, N. A. J., Maury, O., and Barrier, N.: Island restoration to rebuild seabird populations and amplify coral reef functioning, *Conserv. Biol.*, 39, 1–12, <https://doi.org/10.1111/cobi.14313>, 2025.
- 620 Ellis, J. C.: Marine birds on land: A review of plant biomass, species richness, and community composition in seabird colonies, *Plant Ecol.*, 181, 227–241, <https://doi.org/10.1007/s11258-005-7147-y>, 2005.
- Ericsson, T.: Growth and shoot: root ratio of seedlings in relation to nutrient availability, *Plant Soil*, 168–169, 205–214,

- <https://doi.org/10.1007/BF00029330>, 1995.
- 625 Forsberg, P. L., Ernstsen, V. B., Andersen, T. J., Winter, C., Becker, M., and Kroon, A.: The effect of successive storm events and seagrass coverage on sediment suspension in a coastal lagoon, *Estuar. Coast. Shelf Sci.*, 212, 329–340, <https://doi.org/10.1016/j.ecss.2018.07.006>, 2018.
- Foster, C. R., Amos, A. F., and Fuiman, L. A.: Trends in abundance of coastal birds and human activity on a Texas barrier Island over three decades, *Estuaries and Coasts*, 32, 1079–1089, <https://doi.org/10.1007/s12237-009-9224-2>, 2009.
- 630 Le Gouvello, D. Z. M., Nel, R., Harris, L. R., Bezuidenhout, K., and Woodborne, S.: Identifying potential pathways for turtle-derived nutrients cycling through beach ecosystems, *Mar. Ecol. Prog. Ser.*, 583, 49–62, <https://doi.org/10.3354/meps12351>, 2017.
- Hahn, S., Bauer, S., and Klaassen, M.: Estimating the contribution of carnivorous waterbirds to nutrient loading in freshwater habitats, *Freshw. Biol.*, 52, 2421–2433, <https://doi.org/10.1111/j.1365-2427.2007.01838.x>, 2007.
- 635 Heiri, O., Lotter, A. F., and Lemcke, G.: Loss on ignition as a method for estimating organic and carbonate content in sediments : reproducibility and comparability of results, *J. Paleolimnol.*, 25, 101–110, 2001.
- Jones, H. P. and Kress, S. W.: A review of the world’s active seabird restoration projects, *J. Wildl. Manage.*, 76, 2–9, <https://doi.org/10.1002/jwmg.240>, 2012.
- Jones, H. P., Borrelle, S. B., and Rankin, L. L.: Land–sea linkages depend on macroalgal species, predator invasion history in a New Zealand archipelago, *Restor. Ecol.*, 31, 1–11, <https://doi.org/10.1111/rec.13798>, 2023.
- 640 Jones, H. P., Appoo, J., Benkwitt, C. E., Borrelle, S. B., Dunn, R. E., Epstein, H. E., Fowlke, L. A., Holmes, N. D., Jeannot, L., Malhi, Y., and Rankin, L. L.: The circular seabird economy is critical for oceans , islands and people, *Nat. Rev. Biodivers.*, 1–14, <https://doi.org/10.1038/s44358-025-00099-w>, 2025.
- Joyce, M. A., Crotty, S. M., Angelini, C., Cordero, O., Ortals, C., de Battisti, D., and Griffin, J. N.: Wrack enhancement of post-hurricane vegetation and geomorphological recovery in a coastal dune, *PLoS One*, 17, 1–14, <https://doi.org/10.1371/journal.pone.0273258>, 2022.
- 645 Kabat, P., Bazelmans, J., van Dijk, J., Herman, P. M. J., van Oijen, T., Pejrup, M., Reise, K., Speelman, H., and Wolff, W. J.: The Wadden Sea Region: Towards a science for sustainable development, *Ocean Coast. Manag.*, 68, 4–17, <https://doi.org/10.1016/j.ocecoaman.2012.05.022>, 2012.
- Kahmen, A., Perner, J., Audorff, V., Weisser, W., and Buchmann, N.: Effects of plant diversity, community composition and environmental parameters on productivity in montane European grasslands, *Oecologia*, 142, 606–615, <https://doi.org/10.1007/s00442-004-1749-2>, 2005.
- 650 Karasov, W. H.: Digestion in birds: chemical and physiological determinants and ecological implications., *Stud. Avian Biol.*, 13, 1–4, 1990.
- Kim, D. and Lee, K.: Landforms as combined expressions of multiple reciprocally interacting species: Refining the ecosystem engineering concept, *Earth-Science Rev.*, 232, 104152, <https://doi.org/10.1016/j.earscirev.2022.104152>, 2022.
- 655 Koffijberg, K., Frikke, J., Hälterlein, B., Laursen, K., Reichert, G., and Soldaat, L.: Wadden Sea Quality Status Report -

- Breeding birds, Wadden Sea Qual. Status Rep. 2017, 146–147, 2017.
- Kooijman, A. M. and Besse, M.: The higher availability of N and P in lime-poor than in lime-rich coastal dunes in the Netherlands, *J. Ecol.*, 90, 394–403, 2002.
- 660 Kuriyama, Y., Mochizuki, N., and Nakashima, T.: Influence of vegetation on aeolian sand transport rate from a backshore to a foredune at Hasaki, Japan, *Sedimentology*, 52, 1123–1132, <https://doi.org/10.1111/j.1365-3091.2005.00734.x>, 2005.
- Lammers, C., van de Ven, C. N., van der Heide, T., and Reijers, V. C.: Are Ecosystem Engineering Traits Fixed or Flexible: A Study on Clonal Expansion Strategies in Co-occurring Dune Grasses, *Ecosystems*, 26, 1195–1208, <https://doi.org/10.1007/s10021-023-00826-4>, 2023.
- 665 Lansu, E. M., Reijers, V. C., Höfer, S., Luijendijk, A., Rietkerk, M., Wassen, M. J., Lammerts, E. J., and van der Heide, T.: A global analysis of how human infrastructure squeezes sandy coasts, *Nat. Commun.*, 15, 1–7, <https://doi.org/10.1038/s41467-023-44659-0>, 2024.
- Lansu, E. M., Fischman, H. S., Angelini, C., Hijner, N., Geelen, L., Groenendijk, D., Höfer, S., Kooijman, A. M., Rietkerk, M., Tonkens, S., de Vries, S., Wassen, M., van Weerlee, E., Wille, D., Reijers, V., and van der Heide, T.: How human
670 infrastructure threatens biodiversity by squeezing sandy coasts, *Curr. Biol.*, 5210–5219, <https://doi.org/10.1016/j.cub.2025.09.027>, 2025.
- Lausch, A., Jung, A., Bastian, O., Klotz, S., Leitão, P. J., Rocchini, D., and Skidmore, A. K.: Understanding and assessing vegetation health by in situ species and remote-sensing approaches, *Methods Ecol. Evol.*, 9, 1799–1809, <https://doi.org/10.1111/2041-210X.13025>, 2018.
- 675 Lefcheck, J. S.: piecewiseSEM: Piecewise structural equation modelling in r for ecology, evolution, and systematics, *Methods Ecol. Evol.*, 7, 573–579, <https://doi.org/10.1111/2041-210X.12512>, 2016.
- Loder III, T. C., Ganning, B., and Love, J. A.: Ammonia nitrogen dynamics in coastal rockpools affected by gull guano., *J. Exp. Mar. Bio. Ecol.*, 196(1–2), 113–129, 1996.
- van Maanen, B., Coco, G., and Bryan, K. R.: On the ecogeomorphological feedbacks that control tidal channel network
680 evolution in a sandy mangrove setting, *Proc. R. Soc. A Math. Phys. Eng. Sci.*, 471, 20150115, <https://doi.org/10.1098/rspa.2015.0115>, 2015.
- Macreadie, P. I., Anton, A., Raven, J. A., Beaumont, N., Connolly, R. M., Friess, D. A., Kelleway, J. J., Kennedy, H., Kuwae, T., Lavery, P. S., Lovelock, C. E., Smale, D. A., Apostolaki, E. T., Atwood, T. B., Baldock, J., Bianchi, T. S., Chmura, G. L., Eyre, B. D., Fourqurean, J. W., Hall-Spencer, J. M., Huxham, M., Hendriks, I. E., Krause-Jensen, D., Laffoley, D., Luisetti,
685 T., Marbà, N., Masque, P., McGlathery, K. J., Megonigal, J. P., Murdiyarto, D., Russell, B. D., Santos, R., Serrano, O., Silliman, B. R., Watanabe, K., and Duarte, C. M.: The future of Blue Carbon science, *Nat. Commun.*, 10, 1–13, <https://doi.org/10.1038/s41467-019-11693-w>, 2019.
- Marin-Diaz, B., Govers, L. L., Olf, H., and Bouma, T. J.: How grazing management can maximize erosion resistance of salt marshes, *J. Appl. Ecol.*, 58, 1533–1544, <https://doi.org/10.1111/1365-2664.13888>, 2021.
- 690 Maron, J. L., Estes, J. A., Croll, D. A., Danner, E. M., Elmendorf, S. C., and Buckelew, S. L.: An introduced predator alters

- Aleutian Island plant communities by thwarting nutrient subsidies, *Ecol. Monogr.*, 76, 3–24, <https://doi.org/10.1890/05-0496>, 2006.
- McInturf, A. G., Pollack, L., Yang, L. H., and Spiegel, O.: Vectors with autonomy: what distinguishes animal-mediated nutrient transport from abiotic vectors?, *Biol. Rev.*, 94, 1761–1773, <https://doi.org/10.1111/brv.12525>, 2019.
- 695 McKane, R. B., Grigal, D. F., and Russelle, M. P.: Spatiotemporal Differences in ¹⁵N Uptake and the Organization of an Old-Field Plant Community, *Ecology*, 71, 1126–1132, 1990.
- McLeod, E., Chmura, G. L., Bouillon, S., Salm, R., Björk, M., Duarte, C. M., Lovelock, C. E., Schlesinger, W. H., and Silliman, B. R.: A blueprint for blue carbon: Toward an improved understanding of the role of vegetated coastal habitats in sequestering CO₂, *Front. Ecol. Environ.*, 9, 552–560, <https://doi.org/10.1890/110004>, 2011.
- 700 McLoughlin, P. D., Lysak, K., Debeffe, L., Perry, T., and Hobson, K. A.: Density-dependent resource selection by a terrestrial herbivore in response to sea-to-land nutrient transfer by seals, *Ecology*, 97, 1929–1937, <https://doi.org/10.1002/ecy.1451>, 2016.
- Miller, T. E., Gornish, E. S., and Buckley, H. L.: Climate and coastal dune vegetation: Disturbance, recovery, and succession, *Plant Ecol.*, 206, 97–104, <https://doi.org/10.1007/s11258-009-9626-z>, 2010.
- 705 Morton, J. P., Fischman, H. S., Cordero, O., Crabill, J. T., Anthony, M. R., Schneider, M. A., Adams, P. N., and Angelini, C.: Strategic planting and nutrient amendments to accelerate the revegetation of rapidly retreating coastal dunes, *J. Appl. Ecol.*, 62, 267–279, <https://doi.org/10.1111/1365-2664.14859>, 2025.
- Nagy, K. A., Girard, I. A., and Brown, T. K.: Energetics of free-ranging mammals, reptiles, and birds, *Annu. Rev. Nutr.*, 19, 247–277, <https://doi.org/10.1146/annurev.nutr.19.1.247>, 1999.
- 710 Olf, H., Huisman, J., and Toorent, B. F. V. A. N.: Sand Dunes Species dynamics and nutrient accumulation during early primary succession in coastal sand dunes, *J. Ecol.*, 81, 693–706, 1993.
- Otero, X. L., De La Peña-Lastra, S., Pérez-Alberti, A., Ferreira, T. O., and Huerta-Diaz, M. A.: Seabird colonies as important global drivers in the nitrogen and phosphorus cycles, *Nat. Commun.*, 9, 246, <https://doi.org/10.1038/s41467-017-02446-8>, 2018.
- 715 Paleczny, M., Hammill, E., Karpouzi, V., and Pauly, D.: Population trend of the world’s monitored seabirds, 1950–2010, *PLoS One*, 10, 1–11, <https://doi.org/10.1371/journal.pone.0129342>, 2015.
- Pavlik, B. M.: Oecologia Nutrient and productivity relations by nitrogen supply, 233–238, 1983.
- Peña-Lastra, S. D. La, Torre, F., Carballeira, R., Santiso, M. J., Pérez-Alberti, A., and Otero, X. L.: The Rapid Effects of Yellow-Legged Gull (*Larus michahellis*) Colony on Dune Habitats and Plant Landscape in the Atlantic Islands National Park (NW Spain), *Land*, 11, <https://doi.org/10.3390/land11020258>, 2022.
- 720 Pit, I. R., Wassen, M. J., Kooijman, A. M., Dekker, S. C., Griffioen, J., Arens, S. M., and van Dijk, J.: Can sand nourishment material affect dune vegetation through nutrient addition?, *Sci. Total Environ.*, 725, <https://doi.org/10.1016/j.scitotenv.2020.138233>, 2020.
- van de Pol, M., Bailey, L. D., Frauendorf, M., Allen, A. M., van der Sluijs, M., Hijner, N., Brouwer, L., de Kroon, H.,

- 725 Jongejans, E., and Ens, B. J.: Sea-level rise causes shorebird population collapse before habitats drown, *Nat. Clim. Chang.*, 14, 839–844, <https://doi.org/10.1038/s41558-024-02051-w>, 2024.
- Polis, G. A., Anderson, W. B., and Holt, R. D.: Toward an integration of landscape and food web ecology: the dynamics of spatially subsidized food webs., *Annu. Rev. Ecol. Syst.*, 28, 289–316, 1997.
- Poorter, H. and Nagel, O.: The role of biomass allocation in the growth response of plants to different levels of light, CO₂,
730 nutrients and water: a quantitative review., *Funct. Plant Biol.*, 27, 595–607, 2000.
- Raynor, E. J., Pierce, A. R., Leumas, C. M., and Rohwer, F. C.: Breeding habitat requirements and colony formation by royal terns (*thalasseus maximus*) and sandwich terns (*t. Sandvicensis*) on barrier Islands in the gulf of Mexico, *Auk*, 129, 763–772, <https://doi.org/10.1525/auk.2012.11181>, 2012.
- Reijers, V. C., Hoeks, S., van Belzen, J., Siteur, K., de Rond, A. J. A., van de Ven, C. N., Lammers, C., van de Koppel, J., and
735 van der Heide, T.: Sediment availability provokes a shift from Brownian to Lévy-like clonal expansion in a dune building grass, *Ecol. Lett.*, 24, 258–268, <https://doi.org/10.1111/ele.13638>, 2021.
- Reijers, V. C., van Rees, F., van der Heide, T., Oost, A. P., Ruessink, G., Koffijberg, K., Camphuysen, K. C. J., Penning, E., Hijner, N., and Govers, L. L.: Birds influence vegetation coverage and structure on sandy biogeomorphic islands in the Dutch Wadden Sea, *Sci. Total Environ.*, 950, <https://doi.org/10.1016/j.scitotenv.2024.175254>, 2024.
- 740 Riddick, S. N., Dragosits, U., Blackall, T. D., Daunt, F., Wanless, S., and Sutton, M. A.: The global distribution of ammonia emissions from seabird colonies., *Atmos. Environ.*, 55, 319–327, 2012.
- Rijkswaterstaat: LIDAR elevation data of the Dutch coast. Version 1. 4TU.ResearchData. [dataset], <https://doi.org/https://doi.org/10.4121/uuid:8a8a91bc-e520-4d19-a127-5fd2232cc58e>, 2017.
- Savage, C.: Seabird nutrients are assimilated by corals and enhance coral growth rates., *Sci. Rep.*, 9, 4284, 2019.
- 745 Schulte Ostermann, T., Heuner, M., Fuchs, E., Temmerman, S., Schoutens, K., Bouma, T. J., and Minden, V.: Unraveling plant strategies in tidal marshes by investigating plant traits and environmental conditions, *J. Veg. Sci.*, 32, 1–17, <https://doi.org/10.1111/jvs.13038>, 2021.
- Schwarz, C., Gourgue, O., van Belzen, J., Zhu, Z., Bouma, T. J., van de Koppel, J., Ruessink, G., Claude, N., and Temmerman, S.: Self-organization of a biogeomorphic landscape controlled by plant life-history traits, *Nat. Geosci.*, 11, 672–677,
750 <https://doi.org/10.1038/s41561-018-0180-y>, 2018.
- Shiple, B.: Confirmatory path analysis in a generalized multilevel context, *Ecology*, 90, 363–368, <https://doi.org/10.1890/08-1034.1>, 2009.
- Spalding, M. D., Ruffo, S., Lacambra, C., Meliane, I., Hale, L. Z., Shepard, C. C., and Beck, M. W.: The role of ecosystems in coastal protection: Adapting to climate change and coastal hazards, *Ocean Coast. Manag.*, 90, 50–57, <https://doi.org/10.1016/j.ocecoaman.2013.09.007>, 2014.
- 755 Spatz, D. R., Young, L. C., Holmes, N. D., Jones, H. P., VanderWerf, E. A., Lyons, D. E., Kress, S., Miskelly, C. M., and Taylor, G. A.: Tracking the global application of conservation translocation and social attraction to reverse seabird declines., *Proc. Natl. Acad. Sci.*, 120, e2214574120, <https://doi.org/https://doi.org/10.1073/pnas.2214574120>, 2023.

- 760 Stallins, J. A.: Geomorphology and ecology: Unifying themes for complex systems in biogeomorphology, *Geomorphology*, 77, 207–216, <https://doi.org/10.1016/j.geomorph.2006.01.005>, 2006.
- Steibl, S., Bunbury, N., Young, H. S., and Russell, J. C.: A renaissance of atoll ecology., *Annu. Rev. Ecol. Evol. Syst.*, 55, 301–322, 2024.
- 765 Strypsteen, G., de Vries, S., Van Westen, BartBonte, D., Homberger, J.-M., Hallin, C., and Rauwoens, P.: Vertical Growth Rate of Planted Vegetation Controls Dune Growth on a Sandy Beach, *Coast. Eng.*, 194, 104624, <https://doi.org/10.1016/j.coastaleng.2024.104624>, 2024.
- Sutton-Grier, A. E. and Sandifer, P. A.: Conservation of Wetlands and Other Coastal Ecosystems: a Commentary on their Value to Protect Biodiversity, Reduce Disaster Impacts, and Promote Human Health and Well-Being, *Wetlands*, 39, 1295–1302, <https://doi.org/10.1007/s13157-018-1039-0>, 2019.
- 770 Tobias, J. A., Sheard, C., Pigot, A. L., Devenish, A. J. M., Yang, J., Sayol, F., Alioravainen, N., Weeks, T. L., Barber, R. A., Walkden, P. A., Macgregor, H. E. A., Jones, S. E. I., Vincent, C., Phillips, A. G., Marples, N. M., Centellas, F. A. M.-, Silva, V. L.-, Claramunt, S., Darski, B., Freeman, B. G., Bregman, T. P., Cooney, C. R., Hughes, E. C., Capp, E. J. R., Wolfe, J. D., Chapman, P. M., Daly, B. G., Sorensen, M. C., Neu, A., Ford, M. A., Mayhew, R. J., Fabio, L., Kelly, D. J., Annorbah, N. N. D., Pollock, H. S., Zhang, A. M. G.-, Mcentee, J. P., Carlos, J., Meneses, C. G., Muñoz, M. C., and Powell, L. L.: AVONET : morphological , ecological and geographical data for all birds, *Ecol. Lett.*, 25, 581–597, <https://doi.org/10.1111/ele.13898>, 775 2022.
- Tucker, C. J.: Red and photographic infrared linear combinations for monitoring vegetation, *Remote Sens. Environ.*, 8, 127–150, [https://doi.org/10.1016/0034-4257\(79\)90013-0](https://doi.org/10.1016/0034-4257(79)90013-0), 1979.
- 780 van de Ven, C. N., Reijers, V. C., Lammers, C., van Belzen, J., Chung, Y., Bouma, T. J., and van der Heide, T.: Establishing cordgrass plants cluster their shoots to avoid ecosystem engineering, *Funct. Ecol.*, 37, 1339–1349, <https://doi.org/10.1111/1365-2435.14302>, 2023.
- Wainright, S. C., Haney, J. C., Kerr, C., Golovkin, A. N., and Flint, M. V.: Utilization of nitrogen derived from seabird guano by terrestrial and marine plants at St. Paul, Pribilof Islands, Bering Sea, Alaska, *Mar. Biol.*, 131, 63–71, <https://doi.org/10.1007/s002270050297>, 1998.
- 785 Woods, N. N. and Zinnert, J. C.: Shrub encroachment of coastal ecosystems depends on dune elevation, *Plant Ecol.*, 225, 1047–1057, <https://doi.org/10.1007/s11258-024-01453-2>, 2024.
- Young, H. S., McCauley, D. J., and Dirzo, R.: Differential responses to guano fertilization among tropical tree species with varying functional traits, *Am. J. Bot.*, 98, 207–214, <https://doi.org/10.3732/ajb.1000159>, 2011.
- 790 Zarnetske, P. L., Hacker, S. D., Seabloom, E. W., Ruggiero, P., Killian, J. R., Maddux, T. B., and Cox, D.: Biophysical feedback mediates effects of invasive grasses on coastal dune shape, *Ecology*, 93, 1439–1450, <https://doi.org/10.1890/11-1112.1>, 2012.
- Zhang, K., Cao, J., Yin, H., Wang, J., Wang, X., Yang, Y., and Xi, Z.: Microclimate diversity drives grape quality difference at high-altitude: Observation using PCA analysis and structural equation modeling (SEM), *Food Res. Int.*, 191, 114644,

<https://doi.org/10.1016/j.foodres.2024.114644>, 2024.

Zuur, A. F. and Ieno, E. N.: Beginner's guide to spatial, temporal and spatial-temporal ecological. Volume II: GAM and zero-inflated models. data analysis with R-INLA. Volume II: GAM and zero-inflated models., Highland Statistics Ltd., 2018.